BIOCHEMISTRY
including biophysical chemistry & molecular biology
Article

Biochemistry **2010,** *49,* 3631–3639 3631
DOI: 10.1021/bi100160j

Structural Characterization of Mutations at the Oxygen Activation Site in Monomeric Sarcosine Oxidase[†,‡]

Marilyn Schuman Jorns,*[,§] Zhi-wei Chen,[∥] and F. Scott Mathews*[,∥]

[§]*Department of Biochemistry and Molecular Biology, Drexel University College of Medicine, Philadelphia, Pennsylvania 19102, and* [∥]*Department of Biochemistry and Molecular Biophysics, Washington University School of Medicine, St. Louis, Missouri 63110*

Received February 2, 2010; Revised Manuscript Received March 26, 2010

ABSTRACT: Oxygen reduction and sarcosine oxidation in monomeric sarcosine oxidase (MSOX) occur at separate sites above the *si*- and *re*-faces, respectively, of the flavin ring. Mutagenesis studies implicate Lys265 as the oxygen activation site. Substitution of Lys265 with a neutral (Met, Gln, or Ala) or basic (Arg) residue results in an $\sim 10^4$- or 250-fold decrease, respectively, in the reaction rate. The overall structure of MSOX and residue conformation in the sarcosine binding cavity are unaffected by replacement of Lys265 with Met or Arg. The side chain of Met265 exhibits the same configuration in each molecule of Lys265Met crystals and is nearly congruent with Lys265 in wild-type MSOX. The side chain of Arg265 is, however, dramatically shifted (~4−5 Å) compared with Lys265, points in the opposite direction, and exhibits significant conformational variability between molecules of the same crystal. The major species in solutions of Lys265Arg is likely to contain a "flipped-out" Arg265 and exhibit negligible oxygen activation, similar to Lys265Met. The 400-fold higher oxygen reactivity observed with Lys265Arg is attributed to a minor (< 1%) "flipped-in" Arg265 conformer whose oxygen reactivity is similar to that of wild-type MSOX. A structural water (WAT1), found above the *si*-face of the flavin ring in all previously determined MSOX structures, is part of an apparent proton relay system that extends from FAD N(5) to bulk solvent. WAT1 is strikingly absent in Lys265Met and Lys265Arg, a feature that may account for the apparent kinetic stabilization of a reductive half-reaction intermediate that is detectable with the mutants but not wild-type MSOX.

The ability to activate the reduction of molecular oxygen underpins all aerobic biology. Flavoprotein oxidases catalyze the reduction of oxygen to hydrogen peroxide, a highly reactive molecule that, analogous to nitric oxide, is both a cytotoxin and a cell signaling molecule. The mechanism of oxygen activation by flavoprotein oxidases is poorly understood and an area of considerable current interest (*1*−*3*). Recently, we initiated studies of the mechanism of oxygen activation by monomeric sarcosine oxidase (MSOX)[1] (*4*). The enzyme catalyzes the oxidation of sarcosine (*N*-methylglycine) to an imine ($CH_2{=}NH^+CH_2CO_2^-$) that is subsequently hydrolyzed to produce glycine and formaldehyde. MSOX is a 44 kDa two-domain protein that contains covalently bound FAD (8α-*S*-cysteinyl-FAD). The flavin ring of FAD is located at the interface between the flavin and catalytic domains (*5*−*8*). MSOX is a member of a family of monomeric amino acid oxidases (*N*-methyltryptophan oxidase, nikD, pipecolate oxidase, and fructosyl amino acid oxidase) that contain covalently bound FAD (*9*−*13*). MSOX also exhibits structural and sequence homology with the 44 kDa β-subunit of heterotetrameric sarcosine oxidase (TSOX) (*14*, *15*). The TSOX β-subunit contains two flavins: (i) a noncovalently bound FAD that does not react with oxygen but is the site of sarcosine oxidation and is structurally equivalent to the covalent FAD in MSOX and (ii) a covalently bound FMN [8α-(N^3-histidyl)FMN] that is attached to the surface of the β-subunit and the site of oxygen activation (*16*, *17*).

The active site for sarcosine oxidation in MSOX or TSOX is located at highly similar sites above the *re*-face of the flavin ring of FAD (*8*, *14*). Recent mutagenesis studies show that Lys265 is the site of oxygen activation in MSOX and is entirely responsible for the rate acceleration observed with the wild-type enzyme (*4*). Lys265 is located above the *si*-face of the flavin ring and is hydrogen bonded to the N(5) position of FAD via a bridging water molecule (Figure 1). The existence of separate sites for sarcosine oxidation and oxygen reduction on opposite faces of the flavin ring is likely to facilitate the access of oxygen to the reduced flavin by avoiding the sterically crowded region above the *re*-face in the reduced enzyme·imine complex, a catalytically significant intermediate (*7*). Lys265 is absent from the homologous but oxygen-unreactive FAD site in TSOX but is conserved in members of the MSOX family of amino acid oxidases (*10*, *18*, *19*), with the notable exception of nikD. Significantly, ligand-free reduced nikD exhibits low reactivity with oxygen, unlike MSOX. Instead, oxygen activation by nikD is triggered by the presence of bound substrate or product (*20*). Lysine residues hydrogen bonded to flavin N(5) via a bridging water are found in a number of other flavoprotein oxidases (monoamine oxidase B, polyamine oxidase, monoamine oxidase A,

[†]This work was supported in part by Grant GM 31704 (M.S.J.) from the National Institutes of Health.

[‡]Crystallographic coordinates for MSOX mutants have been deposited in the Protein Data Bank (PDB) as entries 3M0O for the phosphate-crystallized Lys265Met mutant, 3M12 for the phosphate-crystallized Lys265Arg mutant, and 3M13 for the PEG-crystallized Lys265Arg mutant.

*To whom correspondence should be addressed. M.S.J.: phone, (215) 762-7495; fax, (215) 762-4452; e-mail, marilyn.jorns@drexelmed.edu. F.S.M.: phone, (314) 362-1080; fax, (314) 362-7183; e-mail, mathews@biochem.wustl.edu.

[1]Abbreviations: FAD, flavin adenine dinucleotide; MSOX, monomeric sarcosine oxidase; TSOX, heterotetrameric sarcosine oxidase; PEG, polyethylene glycol; rmsd, root-mean-square deviation.

Published on Web 03/30/2010

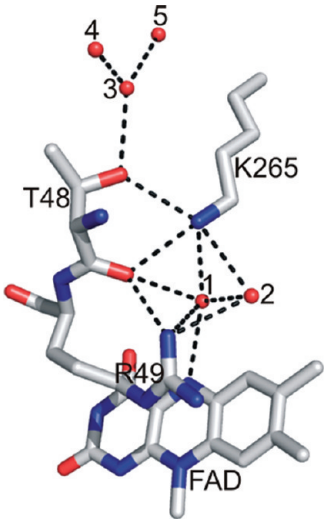

FIGURE 1: View of the region above the *si*-face of the flavin ring in wild-type MSOX (PDB entry 2GBO). Carbons are colored white, oxygens red, and nitrogens blue. Waters are shown as spheres. Waters 3−5 are in contact with bulk solvent. Hydrogen bonds are represented by dashed lines.

L-amino acid oxidase, and lysine-specific histone demethylase) (*21*−*25*). The possible role of these lysines in oxygen activation, however, remains to be determined.

The two-electron reduction of oxygen to hydrogen peroxide by free reduced flavin is thermodynamically favorable but spin-forbidden. Instead, the reaction proceeds via an initial one-electron transfer step that generates a flavin radical−superoxide anion radical pair in a spin-allowed but energetically unfavorable rate-determining step (Scheme 1) (*26*). The rate acceleration observed for the reduction of oxygen by reduced MSOX must clearly be achieved via a decrease in the activation energy ($\Delta G^{\ddagger}$) for the initial one-electron transfer step. $\Delta G^{\ddagger}$ will depend on the free energy change (ΔG) and the reorganization energy (λ) of the reaction. The kinetics observed for the self-exchange reaction between oxygen and superoxide anion indicate that the reoganization energy required to change the configuration of the surrounding medium (λ_{out}) constitutes the major energy barrier in the one-electron reduction of oxygen (*27*). The positively charged ε-amino group of Lys265 and the adjacent pocket occupied by WAT1 and/or WAT2 (see Figure 1) might define a preorganized binding site for superoxide anion that could accelerate the one-electron reduction of oxygen by lowering λ_{out}. Consistent with this scenario, mutation of Lys265 to a neutral residue (Met, Gln, or Ala) results in an $\sim 10^4$-fold decrease in the observed rate of oxygen reduction. Unexpectedly, a chemically conservative substitution of Lys265 with Arg results in a relatively modest but still substantial decrease (250-fold) in the rate of the oxidative half-reaction (*4*). Rapid reaction kinetic studies show that mutation of Lys265 to Met or Arg hardly affects the actual rate of sarcosine oxidation. However, a novel spectral intermediate is observed during the anaerobic reaction of the mutant enzymes with sarcosine. Although the intermediate is not observed with wild-type MSOX, virtually identical spectral properties are observed for substrate-reduced wild-type or mutant enzyme (*4*).

In this paper, we report crystal structures of Lys265Met and Lys265Arg. The results provide considerable insight regarding the observed catalytic properties of the mutant enzymes.

Scheme 1: Reduction of Molecular Oxygen by Reduced Flavin[a]

$$FlH^- + O_2 \xrightarrow{rds} \underset{\text{radical pair}}{[FlH^{\bullet}\ O_2^{\bullet -}]} \longrightarrow Fl_{ox} + HO_2^-$$

[a]Following the initial rate-determining step (rds), conversion of the radical pair to oxidized flavin and hydrogen peroxide may or may not proceed via a 4a-peroxyflavin intermediate (not shown). This intermediate is not detected during oxidative half-reaction studies with MSOX (*4*).

EXPERIMENTAL PROCEDURES

Enzyme Expression and Purification. The Lys265Met and Lys265Arg mutants were expressed and purified as previously described (*4*). The isolated preparations were largely (Lys265Arg) or totally (Lys265Met) devoid of covalently bound FAD. The mutant apoenzymes were reconstituted with FAD to yield preparations containing covalently bound FAD, as previously described (*4*).

Crystallization and Data Collection. Crystals of the Lys265Arg MSOX mutant were grown under two conditions ("phosphate" and "PEG") and those of the Lys265Met mutant under a single condition ("phosphate") by the hanging drop method as described previously (*8*). Equal volumes of 5 μL each of protein solution [10 mg/mL in 20 mM Tris-HCl (pH 8.0)] and reservoir solution [1.7 M Na/K phosphate buffer (pH 7.0) for "phosphate" and ∼20% PEG4000, 200 mM sodium acetate, and 100 mM Tris (pH 8.5) for PEG] were mixed and allowed to equilibrate. X-ray data were recorded from a single crystal from each condition at 100 K, using 15% glycerol as a cryoprotectant for the Lys265Met "phosphate" and the Lys265Arg "PEG" crystals and paratone oil for the Lys265Arg "phosphate" crystal, on an ADSC Quantum-315 CCD detector at Biocars Beamline 14-BM-C at the Advanced Photon Source (Argonne, IL). Spot integration and data scaling were conducted using HKL2000 (*28*, *29*). The space group symmetry, unit cell parameters, contents of the asymmetric units, and data collection statistics are summarized in Table 1.

Structure Determination and Refinement. The initial coordinates of both of the "phosphate" crystals were obtained by direct refinement of the isomorphous wild-type MSOX structure (PDB entry 2GB0), while those of the "PEG" crystal were obtained by molecular replacement using MOLREP from the ccp4 package (*29*), using the same wild-type MSOX structure as the search molecule.

The refinement and electron density map calculations were conducted using REFMAC (*30*), and 5% of the reflections were selected randomly and set aside as a test set for cross validation (*31*). Reflections from 40 Å to the diffraction limit recorded for each data set were included in the refinements, and a bulk solvent correction was applied (*32*). Model building and analysis of the structures were conducted using COOT (*33*). Rigid body refinement followed by several cycles of positional and temperature factor refinement and solvent placement with manual examination were conducted, also using COOT. This procedure utilized electron density difference maps calculated with Fourier coefficients $2F_o - F_c$ and $F_o - F_c$, where F_o and F_c are the observed and calculated structure factors, respectively. The quality of the refined structures and the resulting electron density maps of both structures is high. The final refinement statistics are listed in Table 1.

Structural Calculations and Drawings. Structural diagrams were rendered using PYMOL (http://www.pymol.org).

Table 1: Summary of Data Collection and Refinement for the Lys265Met and Lys265Arg Mutants of MSOX

	Lys265Met ("phosphate")	Lys265Arg ("phosphate")	Lys265Arg ("PEG")
Data Collection			
wavelength (Å)	0.90	0.90	0.90
pH	7.0	7.0	8.5
space group	$P2_1$	$P2_1$	$P2_1$
unit cell dimensions	a = 72.56 Å, b = 69.62 Å, c = 73.98 Å, β = 93.91°	a = 72.32 Å, b = 69.25 Å, c = 73.23 Å, β = 93.68°	a = 99.30 Å, b = 69.30 Å, c = 111.43 Å, β = 93.41°
no. of molecules per asymmetric unit	2	2	4
resolution range (last shell) (Å)	40−1.60 (1.64−1.60)	40−1.60 (1.64−1.60)	40−2.00 (2.18−2.00)
no. of observations	441830	564850	491627
no. of unique observations	92866	93847	83978
redundancy (last shell)	4.8 (3.4)	6.0 (4.7)	5.9 (5.1)
completeness (last shell)	96.2 (85.0)	99.1 (99.1)	95.3 (96.0)
R_{merge}[a] (last shell) (%)	6.6 (43.1)	7.0 (42.7)	7.2 (47.5)
$I/\sigma(I)$[b] (last shell)	17.2 (2.1)	21.7 (2.9)	21.0 (3.2)
Refinement			
resolution (Å)	40−1.6	40−1.6	40−2.1
R_{cryst}[c]	0.173	0.179	0.187
R_{free}[d]	0.208	0.215	0.248
no. of reflections (working/test)	88220/4626	89125/4704	79550/4212
no. of protein atoms	6053	6019	11912
no. of water molecules	713	792	497
FAD/Cl	2/2	2/2	4/4
rmsd for bond lengths[e] (Å)	0.011	0.007	0.023
rmsd for bond angles[e] (deg)	1.4	1.1	2.0
rms ΔB (Å^2) (mm/ms/ss)[f]	0.73/0.58/2.22	0.56/0.44/1.38	1.16/0.94/3.08
$\langle B \rangle$ for protein (Å^2)	19.9	19.3	37.2
$\langle B \rangle$ for water molecules (Å^2)	32.6	26.2	38.5
$\langle B \rangle$ for FAD/Cl/PO_4	14.3/15.4/0	13.8/14.2/0	28.4/29.3/2
no. of residues in alternate conformations[g]	4	4	0
Ramachandran plot (%)			
preferred region	99.5	99.5	99.7
allowed region	0.2	0.2	0.0
disallowed region	0.3	0.3	0.3

[a] $R_{merge} = \sum_h \sum_i I(h) - I_i(h) \leftrightarrows \sum_h \sum_i I_i(h)$, where $I_i(h)$ and $I(h)$ are the ith and mean measurements of reflection h, respectively. [b] $I/\sigma(I)$ is the average signal-to-noise ratio for merged reflection intensities. [c] $R = \sum_h |F_o - F_c| / \sum_h |F_o|$, where F_o and F_c are the observed and calculated structure factor amplitudes of reflection h, respectively. [d] R_{free} is the test reflection data set, ~5% selected randomly for cross validation during crystallographic refinement (*31*). [e] Deviations from ideal bond lengths and angles and B factors of bonded atoms. [f] mm, main chain to main chain; ms, main chain to side chain; ss, side chain to side chain. [g] For Lys265Met ("phosphate"), the residues in an alternate conformation are AGlu141, AArg154, ASer191, and BGlu141; for Lys265Arg ("phosphate"), the residues in an alternate conformation are AAsp47, AArg154, ASer358, and BAsp47.

RESULTS

Overall Structure of the Mutant Enzymes and Comparison with Wild-Type MSOX. The Lys265Met mutant was crystallized under precipitating conditions of high salt to produce "phosphate" crystals that diffract to 1.6 Å and contain two molecules in the asymmetric unit. When the two molecules in the crystals are aligned, the only significant differences in backbone structure are found in an external loop (Ile185−Tyr192) and an active site loop (Tyr55−Tyr61) (Figure 2). Previous studies with "phosphate" crystals of other MSOX preparations show that the configuration of the external loop is sensitive to the crystal packing environment and is consistently different between molecule 1 (A configuration) and molecule 2 (B configuration) in the asymmetric unit (*34*). The same pattern is observed with phosphate crystals of Lys265Met (Table 2). The active site loop controls access to a solvent-filled active site cavity above the *re*-face of the flavin ring. The active site loop is found in the closed configuration in complexes of the wild-type enzyme with various sarcosine analogues (*6*, *8*). In contrast, the active site loop is mobile in ligand-free MSOX, as judged by the open and closed configurations observed in molecules 1 and 2, respectively, in "phosphate" crystals of the wild-type enzyme or Lys265Met (Table 2). Importantly, no significant difference in backbone structure is detected when molecule 1 or 2 in Lys265Met "phosphate" crystals is compared with the corresponding molecule in wild-type "phosphate" crystals (data not shown) (see Figure S1 of the Supporting Information).

The Lys265Arg mutant was crystallized in the presence of high salt ("phosphate" crystals) to produce crystals that diffract to 1.6 Å and contain two molecules in the asymmetric unit. Molecules 1 and 2 in "phosphate" Lys265Arg crystals exhibit configurations of the external and active site loops that are identical to those observed for the wild-type enzyme (Table 2). Very similar backbone structures are apparent upon comparison of molecule 1 or 2 in the mutant crystals with the corresponding molecule in the wild-type crystal (data not shown) [see Figure S2 (top and middle panels) of the Supporting Information].

The Lys265Arg mutant was also crystallized in the presence of high PEG ("PEG" crystals) to produce crystals that diffract to 2.1 Å and contain four molecules in the asymmetric unit. The four molecules in the "PEG" crystals of Lys265Arg exhibit an A or A-like configuration of the external loop, similar to that observed

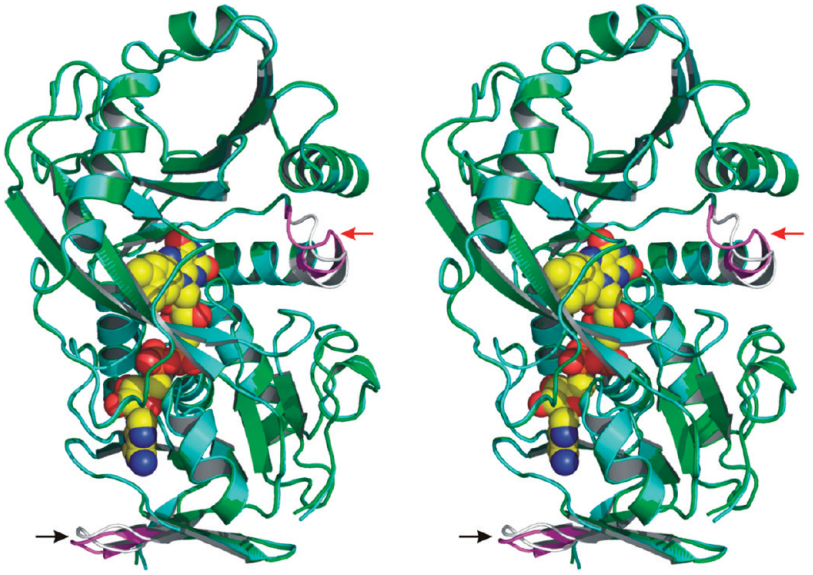

FIGURE 2: Stereo ribbon drawing comparing the two molecules in "phosphate" crystals of Lys265Met. Molecule 1 is shown as a green ribbon, except for the white active site and external loops. Molecule 2 is shown as a cyan ribbon, except for the magenta active site and external loops. FAD is shown as a space-filling model with carbon, nitrogen, and oxygen atoms colored yellow, blue, and red, respectively. The active site and external loops are denoted by red and black arrows, respectively.

Table 2: Comparison of Lys265Met or Lys265Arg Crystals with Wild-Type MSOX or Arg49Lys Crystals

crystal							comparison with wild type[a] [rmsd (Å)]	
enzyme	precipitant	resolution (Å)	molecule	active site loop (Y55−Y61)	Arg52	external loop (I185−Y192)	molecule 1	molecule 2
wild type[b]	phosphate	1.85	1	open	out	A configuration		
			2	closed	out and in-like	B configuration		
Lys265Met	phosphate	1.6	1	open	out	A configuration	0.16	
			2	closed	in	B configuration		0.13
Lys265Arg	phosphate	1.6	1	open	out	A configuration	0.21	
			2	closed	in	B configuration		0.19
Lys265Arg	PEG	2.1	1	open	out	A configuration	0.33	
			2	open	out	A-like configuration	0.31	
			3	open	out	A-like configuration	0.33	
			4	open	out	A-like configuration	0.29	
Arg49Lys[c]	phosphate	1.70	1	closed	in	A configuration	0.34	0.37
			2	closed	in	B configuration		0.15
Arg49Lys[d]	PEG	2.10	1	open	out	A configuration	0.21	
			2	closed	in	A configuration	0.38	0.39

[a]Comparison is made between molecules in mutant and wild-type crystals that exhibit the same configuration for the active site and external loops. If the latter is not possible, the molecule in the mutant crystal is compared with each of the two molecules in wild-type crystals. [b]PDB entry 2GBO. [c]PDB entry 3BHK. [d]PDB entry 3BHF.

with "PEG" crystals of Arg49Lys (*34*). The results are consistent with an altered packing arrangement in "PEG" crystals as compared to "phosphate" crystals. The active site loop is in the open configuration in each of the four molecules in "PEG" Lys265Arg crystals, whereas PEG crystals of Arg49Lys exhibit both open and closed configurations (Table 2). Except for minor variations in the external loop, no significant difference in backbone structure is detected upon comparison of molecule 1, 2, 3, or 4 in "PEG" Lys265Arg crystals with molecule 1 in "phosphate" wild-type crystals (data not shown) [see Figure S2 (bottom panel) of the Supporting Information].

Does Mutation of Lys265 Affect the Structure of the Sarcosine Oxidation Site? The active site cavity for sarcosine oxidation is located above the *re*-face of the flavin ring. When the active site loop is in the open configuration, the cavity in ligand-free wild-type MSOX contains eight water molecules (WAT1−8) and Arg52 is found in the "out" position (Figure 3). WAT1−5 occupy the sarcosine binding site and are displaced upon binding of substrate analogues (*35*). Formation of a complex also results in closure of the active site loop, movement of Arg52 from the "out" to the "in" position, and displacement of two additional waters (WAT6 and WAT7), probably caused by the accompanying motion of Arg52. Only a single water molecule (WAT8) is retained in MSOX complexes with substrate analogues. The structures observed for these complexes indicate that the substrate carboxylate group is bound to Lys348 and Arg52. The carbonyl oxygen of Gly344 forms a hydrogen bond to the NH group in sarcosine (*6*, *8*). His269 and Tyr317 are important for optimizing the orientation of the bound substrate (*36*, *37*).

Comparison of molecule 1 in "phosphate" Lys265Met crystals with molecule 1 in the corresponding wild-type crystals indicates that the active site cavity is scarcely affected by the mutation.

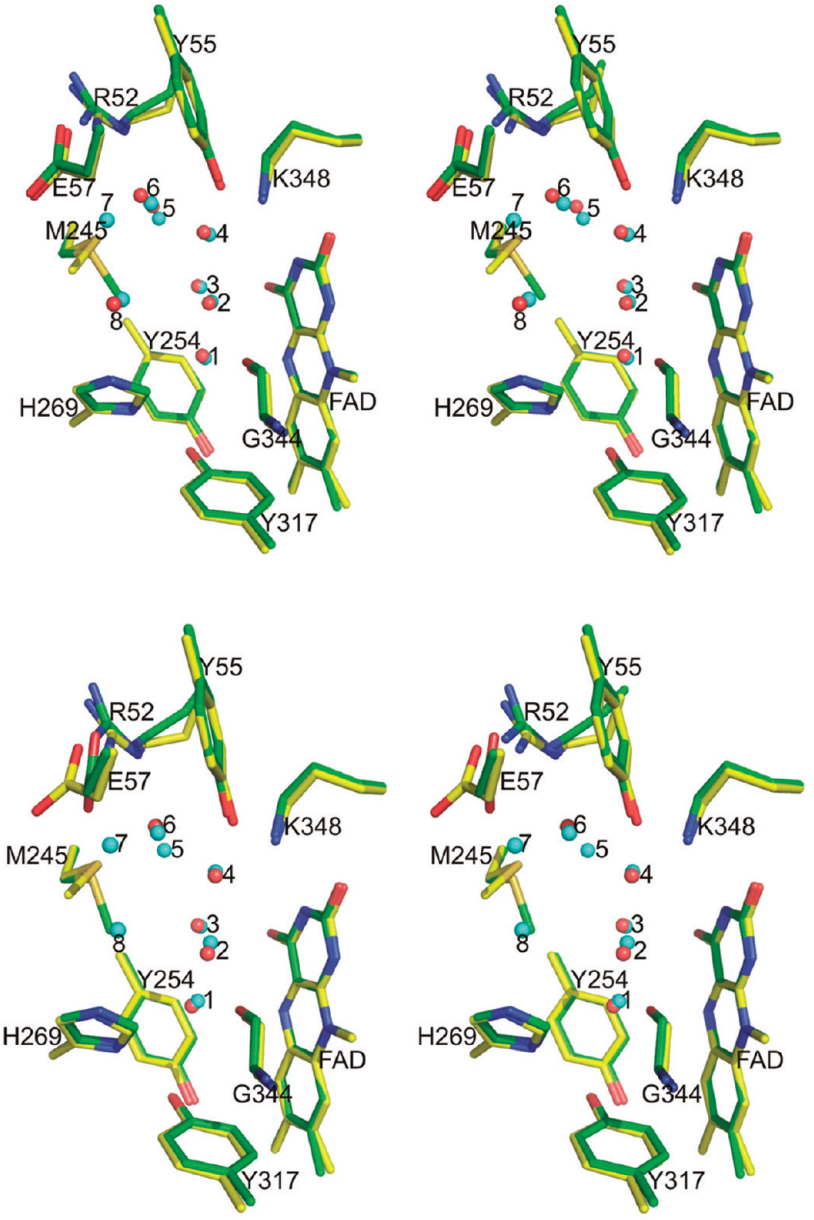

FIGURE 3: Stereoview comparison of the sarcosine oxidation site above the *re*-face of the flavin ring in Lys265Met or Lys265Arg with wild-type MSOX (PDB entry 2GBO). Oxygen and nitrogen atoms are colored red and blue, respectively, except for water molecules in wild-type MSOX (WAT1−8) which are shown as cyan spheres. The top panel compares molecule 1 in Lys265Met "phosphate" crystals (green carbons) with molecule 1 in wild-type MSOX "phosphate" crystals (yellow carbons). The bottom panel compares molecule 1 in Lys265Arg "phosphate" crystals (green carbons) with molecule 1 in wild-type MSOX "phosphate" crystals (yellow carbons).

Two changes are, however, worth noting. (i) WAT7 is not detected in the mutant structure, and (ii) there is a 2.4 Å shift in the position of Met245 CE (Figure 3, top panel). The active site cavity in Lys265Arg is also largely unperturbed, which can be seen by the structure observed for molecule 1 in "phosphate" crystals (Figure 3, bottom panel). However, in this case, two additional water molecules are absent in the mutant crystals (WAT5 and WAT8) and an additional side chain atom, Glu57 OE(2), is shifted by 1.8 Å. Similar results were obtained for molecules 1−4 in "PEG" Lys265Arg crystals (data not shown).

Does Mutation of Lys265 Cause Structural Changes above the si-Face of the Flavin Ring? Oxygen activation in wild-type MSOX occurs at Lys265, a residue located above the *si*-face of the flavin ring. Lys265 NZ is hydrogen bonded to FAD N(5) via a bridging water molecule (WAT1). WAT1 is also hydrogen bonded to Arg49 NH(1), Thr48 O, and a second water molecule (WAT2). Arg49 is in van der Waals contact with the *si*-face of the flavin ring (Figure 4). Thr48 is part of a putative proton relay system extending from FAD N(5) to bulk solvent (see Figure 1). WAT1 is present in all previously determined MSOX structures, including both molecules found in "phosphate" crystals of the wild-type enzyme (2GBO), His269Asn (1L9C), Arg49Lys (3BHF), or complexes of wild-type MSOX with various inhibitors (1EL9, 1EL1, 2GF3, and 1EL5) and both molecules in "PEG" crystals of Arg49Lys (3BHF). Five of the eight crystals also contain WAT2 in both molecules (2GBO, 1L9C, 2GF3, 3BHF, and 1EL5), whereas the others (1EL9, 1EL1, and 3BHK) contain WAT2 in one of the two molecules.

Molecules 1 and 2 in "phosphate" crystals of Lys265Met exhibit identical conformations for residues above the *si*-face of FAD. Importantly, the side chain of Met265 is nearly congruent to that of Lys265 in wild-type MSOX, except for a 1.6 Å difference

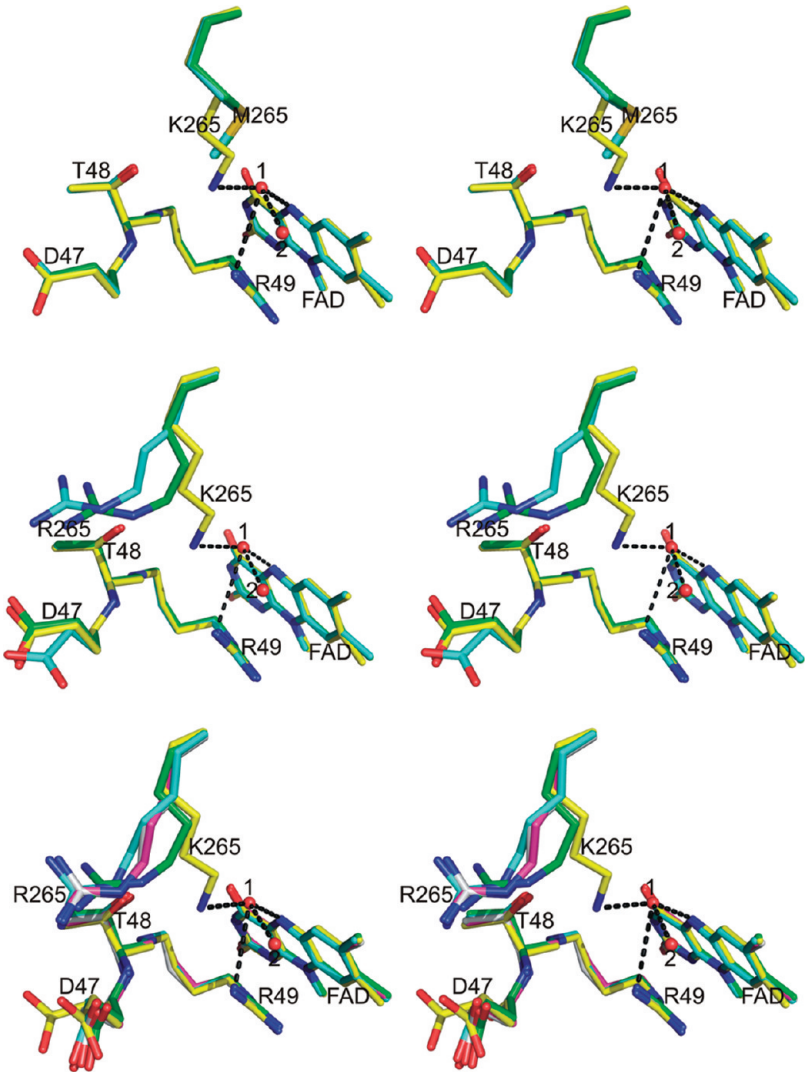

FIGURE 4: Stereoview comparison of the region above the *si*-face of the flavin ring in Lys265Met or Lys265Arg with wild-type MSOX (PDB entry 2GBO). Two water molecules, shown as red spheres in each panel, are found in wild-type MSOX but not in the two Lys265 mutants. The two alternate conformations of Asp47 (A and B) found in wild-type MSOX molecule 1 are shown in the bottom panel; only the A conformation is shown in the top and middle panels. Selected hydrogen bonds are represented by dashed lines. The top panel compares molecules 1 and 2 in "phosphate" Lys265Met crystals (green and cyan carbons, respectively) with molecule 1 in wild-type MSOX (yellow carbons). The middle panel compares molecules 1 and 2 in "phosphate" Lys265Arg crystals (green and cyan carbons, respectively) with molecule 1 in wild-type MSOX (yellow carbons). For the sake of clarity, only the A and A-like conformations of Asp47 are shown for molecules 1 and 2, respectively, in the mutant enzyme. The bottom panel compares molecules 1−4 in "PEG" Lys265Arg crystals (green, magenta, cyan, and white carbons, respectively) with molecule 1 in wild-type MSOX (yellow carbons).

between the position of the sulfur atom in Met265 and the corresponding carbon atom in Lys265. In wild-type MSOX, two alternate conformations for Asp47 are observed in molecule 1 (A and B). Only the A conformation of Asp47 is found in molecule 2 of wild-type MSOX or in both molecules of "phosphate" crystals of Lys265Met. Thr48 and Arg49 occupy identical positions in the wild-type and mutant enzyme, but WAT1 and WAT2 are strikingly absent in both molecules of the mutant crystals. Aside from this difference, the region above the *si*-face of the flavin is virtually unaffected by mutation of Lys265 to Met (Figure 4, top panel). Figure S3 (top panel) of the Supporting Information shows $2F_o - F_c$ and $F_o - F_c$ electron density maps for selected residues above the *si*-face in molecule 1 of "phosphate" crystals of Lys265Met.

A dramatic effect on the conformation and flexibility of the side chain of residue 265 is observed upon mutation of Lys265 to Arg, as judged by results obtained for the two molecules in "phosphate" crystals or the four molecules in "PEG" crystals of Lys265Met (Figure 4, middle and bottom panels, respectively). The side chain of Arg265 has moved ~4−5 Å away from FAD and points in a significantly different direction, as compared with Lys265 in wild-type MSOX. Unlike Lys265 or Met265, the side chain of Arg265 exhibits substantial mobility, as judged by a distance of 1−2 Å observed between equivalent atoms when molecules in the same crystal are aligned with each other. Two alternate conformations for Asp47 are observed in molecule 1 (A-like and B-like) or molecule 2 (A-like and B-like) in "phosphate" crystals of Lys265Arg. Only the B conformation of Asp47 is found in molecules 1−4 in "PEG" crystals of Lys265Arg. Mutation of Lys265 to Arg does not affect the conformation of Arg49 or Thr48 but does result in the apparent loss of the two *si*-face waters (WAT1 and WAT2) that are found in crystals of wild-type MSOX but not Lys265Met (Figure 4). Figure S3 (bottom panel) of the Supporting Information shows $2F_o - F_c$ and $F_o - F_c$ electron density maps for selected residues above the *si*-face in molecule 1 of "phosphate" crystals of Lys265Arg.

Scheme 2: Proposed Mechanism for the Reduction of MSOX by Sarcosine[a]

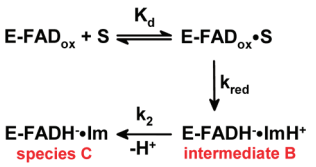

[a]Abbreviations: S, sarcosine; ImH^+, protonated sarcosine imine; Im, unprotonated sarcosine imine.

The corresponding data for molecules 1 and 3 of "PEG" crystals of Lys265Arg are shown in Figure S4 of the Supporting Information.

DISCUSSION

Mutation of Lys265 to Met results in an ~10^4-fold decrease in the rate of the reaction of reduced MSOX with oxygen (*4*). The mutation does not affect the overall structure of the enzyme. The conformation of residues at the active site for sarcosine oxidation and the proposed oxygen activation site on the opposite face of the flavin ring are nearly identical in Lys265Met and wild-type MSOX. The results provide compelling evidence that the enormous decrease in oxygen reactivity observed with Lys265Met is attributable to the loss of a basic residue at position 265 that is likely to provide a preorganized binding site for superoxide anion. A chemically conservative mutation of Lys265 to Arg results in a relatively modest but still substantial decrease (250-fold) in the rate of oxygen reduction (*4*). The overall structure of Lys265Arg and the configuration of residues at its two active sites are virtually identical to those of wild-type MSOX, with the notable exception of the mutated residue. In Lys265Met, the side chain of residue 265 is nearly congruent with that of Lys265 in the wild-type enzyme and exhibits the same configuration in each molecule of the mutant crystals. In sharp contrast, substitution of Lys265 with Arg has a profound effect on the position and mobility of the mutated residue. The side chain of Arg265 is shifted by ~4−5 Å as compared with Lys265, points away from the flavin ring, and exhibits significant conformational variability in different molecules within the same crystal. The accessible surface area of an arginine residue in a peptide (225 $Å^2$) is ~10% larger than for lysine (200 $Å^2$) (*38*). The observed local structural perturbation suggests that the side chain of Arg265 is not readily accommodated in the space occupied by Lys265 in wild-type MSOX. The structures observed for "phosphate" or "PEG" Lys265Arg crystals strongly suggest that molecules containing a "flipped-out" Arg265 will comprise the major species in solution. These molecules are likely to exhibit negligible oxygen activation, similar to that observed upon mutation of Lys265 to a neutral residue. We postulate that the 400-fold higher oxygen reactivity observed with Lys265Arg compared with mutants lacking a basic residue at position 265 is attributable to a minor (<1%) "flipped-in" conformer of Arg265 that exhibits oxygen reactivity similar to that of wild-type MSOX.

Mutation of Lys265 to Met or Arg causes only a very modest decrease (~5-fold) in the rate of sarcosine oxidation (Scheme 2, k_{red}) (*4*), consistent with the observed structural integrity of the active site cavity above the *re*-face of the flavin ring. However, sarcosine oxidation by the mutant enzymes results in the formation of a novel intermediate (B) that exhibits an absorption spectrum significantly different from that expected for a two-electron reduced flavin (Figure 5, curve 2). Intermediate B undergoes an apparent first-order conversion to a final reduced

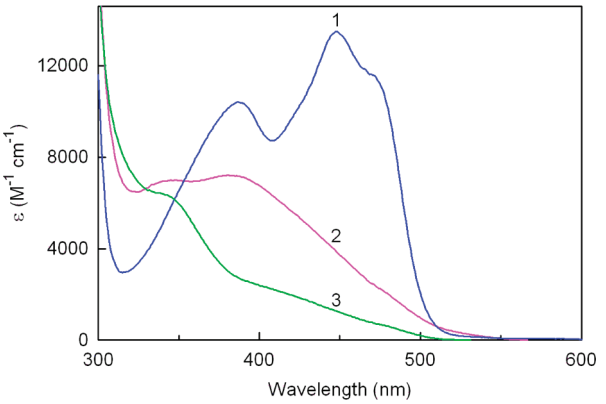

FIGURE 5: Curve 1 is the absorption spectrum of oxidized Lys265Met. Curve 3 is the final absorption spectrum of reduced Lys265Met (species C) observed after anaerobic reaction with 140 mM sarcosine in 100 mM potassium phosphate buffer (pH 8.0) at 25 °C. Curve 2 is the calculated absorption spectrum of intermediate B. The data were taken from ref *4*. Similar results were obtained with Lys265Arg (*4*).

species (C) (Scheme 2, k_2) that exhibits a typical fully reduced flavin spectrum (Figure 5, curve 3) (*4*). Intermediate B is not detected during reduction of wild-type MSOX (*35*). The absorption spectrum of the substrate-reduced wild-type enzyme is, however, virtually identical to that observed for species C with the Lys265 mutants. The results strongly suggest that intermediate B is also formed during reduction of wild-type MSOX but is not detectable because of a much faster conversion of the intermediate to species C (i.e., $k_2 \geq 20k_{red}$). The value obtained for k_2 with Lys265Met or Lys265Arg is ~25-fold slower than the value observed for k_{red} with wild-type MSOX (*4*, *35*). This analysis indicates that the Lys265 mutations probably cause an at least 500-fold decrease in the rate of conversion of intermediate B to species C.

MSOX oxidizes the anionic form of sarcosine ($CH_3NHCH_2CO_2^-$) (*37*). Transfer of a hydride equivalent from the substrate methyl group to N(5) of FAD will generate a reduced enzyme complex with the protonated form of sarcosine imine ($EFADH^- \cdot CH_2{=}NH^+CH_2CO_2^-$). Charge transfer interaction between the electron-rich 1,5-dihydroflavin anion and the positively charged imimium group could account for the "atypical" absorption spectrum observed for intermediate B. Interestingly, a spectrally similar intermediate has been observed with the wild-type forms of at least two other flavoprotein oxidases (dimethylglycine oxidase and alditol oxidase) and analogously attributed to a reduced enzyme·product complex (*39*, *40*).

Release of the protonated imine from intermediate B would eliminate charge transfer interaction and might account for the spectral properties observed for species C. Two sets of data, however, indicate that species C cannot be the free reduced enzyme. (i) Species C is formed at a catalytically significant rate during reduction of wild-type MSOX (*35*). Steady-state kinetics studies indicate that a reduced enzyme·imine complex is the species that reacts with oxygen (*7*). (ii) Conversion of intermediate B to species C is estimated to be at least 500-fold slower with the mutant enzymes. If this step involved product release, the mutant enzymes should exhibit a large decrease in the binding affinity for the substrate or substrate analogues. The latter is not expected on the basis of the observed structural integrity of the sarcosine binding site, nor is it consistent with the very modest decrease (<5-fold) in stability observed for complexes of the mutant enzymes with sarcosine or methylthioacetate (*4*).

Mutation of Lys265 to Met or Arg results in the apparent loss of two water molecules on the *si*-face of the flavin ring. WAT1 forms part of an apparent proton relay system that extends from the N(5) position of FAD to bulk solvent (see Figure 1). WAT1 is found in each molecule of all previously determined structures of wild-type MSOX and two other mutants. We propose that conversion of intermediate B to species C involves ionization of the protonated sarcosine imine (Scheme 2), a step that would eliminate charge transfer interaction between the reduced flavin and the imine. Importantly, proton release is likely to be at least 100-fold slower in the Lys265 mutants, as judged by results obtained upon disruption of a proton relay network in dihydroorotate dehydrogenase (*41*). Experiments for evaluating this structure-based mechanism will be part of future studies.

Concluding Remarks. Mutation of Lys265 to Met or Arg results in the elimination or displacement of a positive charge from a pocket above the *si*-face of the flavin ring. This results in the loss of a charge-stabilized preformed binding site for the superoxide anion, an intermediate in the oxidative half-reaction of MSOX, and a greatly reduced rate of oxygen reduction. At the same time, the mutations disrupt a water relay system near the flavin N(5) atom that probably catalyzes the ionization of a protonated sarcosine intermediate, leading to a transient accumulation of a charge transfer intermediate along the pathway of product release from the reoxidized enzyme.

ACKNOWLEDGMENT

We thank Gouhua Zhao for his help in the preparation of the mutant enzymes.

SUPPORTING INFORMATION AVAILABLE

Stereo ribbon drawings of Lys265Met and wild-type MSOX (Figure S1), stereo ribbon drawings of Lys265Arg and wild-type MSOX (Figure S2), electron density maps for selected residues in "phosphate" crystals of Lys265Met or Lys265Arg (Figure S3), and electron density maps for selected residues in "PEG" crystals of Lys265Arg (Figure S4). This material is available free of charge via the Internet at http://pubs.acs.org.

REFERENCES

1. Mattevi, A. (2006) To be or not to be an oxidase: Challenging the oxygen reactivity of flavoenzymes. *Trends Biochem. Sci. 31*, 276–283.
2. Baron, R., McCammon, J. A., and Mattevi, A. (2009) The oxygen-binding vs. oxygen-consuming paradigm in biocatalysis: Structural biology and biomolecular simulation. *Curr. Opin. Struct. Biol. 19*, 672–679.
3. Klinman, J. P. (2007) How do enzymes activate oxygen without inactivating themselves? *Acc. Chem. Res. 40*, 325–333.
4. Zhao, G., Bruckner, R. C., and Jorns, M. S. (2008) Identification of the oxygen activation site in monomeric sarcosine oxidase: Role of Lys265 in catalysis. *Biochemistry 47*, 9124–9135.
5. Wagner, M. A., Khanna, P., and Jorns, M. S. (1999) Structure of the flavocoenzyme of two homologous amine oxidases: Monomeric sarcosine oxidase and N-methyltryptophan oxidase. *Biochemistry 38*, 5588–5595.
6. Wagner, M. A., Trickey, P., Chen, Z., Mathews, F. S., and Jorns, M. S. (2000) Monomeric sarcosine oxidase. 1. Flavin reactivity and active site binding determinants. *Biochemistry 39*, 8813–8824.
7. Wagner, M. A., and Jorns, M. S. (2000) Monomeric sarcosine oxidase. 2. Kinetic studies with sarcosine, alternate substrates and substrate analogs. *Biochemistry 39*, 8825–8829.
8. Trickey, P., Wagner, M. A., Jorns, M. S., and Mathews, F. S. (1999) Monomeric sarcosine oxidase: Structure of a covalently-flavinylated secondary amine oxidizing enzyme. *Structure 7*, 331–345.
9. Khanna, P., and Jorns, M. S. (2001) Characterization of the FAD-containing N-methyltryptophan oxidase from *Escherichia coli*. *Biochemistry 40*, 1441–1450.
10. Ilari, A., Bonamore, A., Franceschini, S., Fiorillo, A., Boffi, A., and Colotti, G. (2008) The X-ray structure of N-methyltryptophan oxidase reveals the structural determinants of substrate specificity. *Proteins 71*, 2065–2075.
11. Carrell, C. J., Bruckner, R. C., Venci, D., Zhao, G., Jorns, M. S., and Mathews, F. S. (2007) NikD, an unusual amino acid oxidase essential for nikkomycin biosynthesis: Structures of closed and open forms at 1.15 and 1.90 Å resolution. *Structure 15*, 928–941.
12. Dodt, G., Kim, D. G., Reimann, S. A., Reuber, B. E., McCabe, K., Gould, S. J., and Mihalik, S. J. (2000) L-Pipecolic acid oxidase, a human enzyme essential for the degradation of L-pipecolic acid, is most similar to the monomeric sarcosine oxidases. *Biochem. J. 345*, 487–494.
13. Collard, F., Zhang, J., Nemet, I., Qanungo, K. R., and Monnier, V. M. (2008) Crystal structure of the deglycating enzyme fructosamine oxidase (amadoriase II). *J. Biol. Chem. 283*, 27007–27016.
14. Chen, Z., Hassan-Abdallah, A., Zhao, G., Jorns, M. S., and Mathews, F. S. (2006) Heterotetrameric sarcosine oxidase: Structure of a diflavin metalloenzyme at 1.85 Å resolution. *J. Mol. Biol. 360*, 1000–1018.
15. Chlumky, L. J., Zhang, L., and Jorns, M. S. (1995) Sequence analysis of sarcosine oxidase and nearby genes reveals homologies with key enzymes of folate one-carbon metabolism. *J. Biol. Chem. 270*, 18252–18259.
16. Willie, A., Edmondson, D. E., and Jorns, M. S. (1996) Sarcosine oxidase contains a novel covalently bound FMN. *Biochemistry 35*, 5292–5299.
17. Kvalnes-Krick, K., and Jorns, M. S. (1986) Bacterial sarcosine oxidase: Comparison of two multisubunit enzymes containing both covalent and noncovalent flavin. *Biochemistry 25*, 6061–6069.
18. Reuber, B. E., Karl, C., Reimann, S. A., Mihalik, S. J., and Dodt, G. (1997) Cloning and functional expression of a mammalian gene for a peroxisomal sarcosine oxidase. *J. Biol. Chem. 272*, 6766–6776.
19. Miura, S., Ferri, S., Tsugawa, W., Kiin, S., and Sode, K. (2006) Active site analysis of fructosyl amine oxidase using homology modeling and site-directed mutagenesis. *Biotechnol. Lett. 28*, 1895–1900.
20. Kommoju, P. R., Bruckner, R. C., Ferreira, P., Carrell, C. J., Mathews, F. S., and Jorns, M. S. (2009) Factors that affect oxygen activation and coupling of the two redox cycles in the aromatization reaction catalyzed by nikD, an unusual amino acid oxidase. *Biochemistry 48*, 9542–9555.
21. Binda, C., Li, M., Hubalek, F., Restelli, N., Edmondson, D. E., and Mattevi, A. (2003) Insights into the mode of inhibition of human mitochondrial monoamine oxidase B from high-resolution crystal structures. *Proc. Natl. Acad. Sci. U.S.A. 100*, 9750–9755.
22. Binda, C., Coda, A., Angelini, R., Federico, R., Ascenzi, P., and Mattevi, A. (1999) A 30 angstrom long U-shaped catalytic tunnel in the crystal structure of polyamine oxidase. *Structure 7*, 265–276.
23. Son, S., Ma, J., Kondou, Y., Yoshimura, M., Yamashita, E., and Tsukihara, T. (2008) Structure of human monoamine oxidase A at 2.2 Å resolution: The control of opening the entry for substrates/inhibitors. *Proc. Natl. Acad. Sci. U.S.A. 105*, 5739–5744.
24. Pawelek, P. D., Cheah, J., Coulombe, R., Macheroux, P., Ghisla, S., and Vrielink, A. (2000) The structure of L-amino acid oxidase reveals the substrate trajectory into an enantiomerically conserved active site. *EMBO J. 19*, 4204–4215.
25. Chen, Y., Yang, Y., Wang, F., Wan, K., Yamane, K., Zhang, Y., and Lei, M. (2006) Crystal structure of human histone lysine-specific demethylase 1 (LSD1). *Proc. Natl. Acad. Sci. U.S.A. 103*, 13956–13961.
26. Massey, V. (1994) Activation of molecular oxygen by flavins and flavoproteins. *J. Biol. Chem. 269*, 22459–22462.
27. Lind, J., Shen, X., Merenyi, G., and Jonsson, B. O. (1989) Determination of the rate constant of self-exchange of the $O_2/O_2^{\bullet-}$ couple in water by $^{18}O/^{16}O$ isotope marking. *J. Am. Chem. Soc. 111*, 7654–7655.
28. Otwinowski, Z., and Minor, W. (1997) Processing of X-ray diffraction data collected in oscillation mode. *Methods Enzymol. 276*, 307–326.
29. Collaborative Computational Project Number 4 (1994) *Acta Crystallogr. D50*, 760–763.
30. Murshudov, G., Vagin, A., and Dodson, E. (1997) Refinement of macromolecular structures by the maximum likelyhood method. *Acta Crystallogr. D53*, 240–255.
31. Kleywegt, G. J., and Brünger, A. T. (1996) Checking your imagination: Application of the free r value. *Structure 4*, 897–904.
32. Jiang, J.-S., and Brünger, A. T. (1994) Protein hydration observed by X-ray diffraction. Solvation properties of penicillopepsin and neuraminidase crystal structures. *J. Mol. Biol. 243*, 100–115.
33. Emsley, P., and Cowtan, K. (2004) Coot: Model-building tools for molecular graphics. *Acta Crystallogr. D60*, 2126–2132.

34. Hassan-Abdallah, A., Zhao, G., Chen, Z., Mathews, F. S., and Jorns, M. S. (2008) Arg49 is a bifunctional residue important in catalysis and biosynthesis of monomeric sarcosine oxidase: A context-sensitive model for the electrostatic impact of arginine to lysine mutations. *Biochemistry 47*, 2913–2922.
35. Zhao, G., and Jorns, M. S. (2006) Spectral and kinetic characterization of the Michaelis charge transfer complex in monomeric sarcosine oxidase. *Biochemistry 45*, 5985–5992.
36. Zhao, G., Song, H., Chen, Z., Mathews, F. S., and Jorns, M. S. (2002) Monomeric sarcosine oxidase: Role of histidine 269 in catalysis. *Biochemistry 41*, 9751–9764.
37. Zhao, G., and Jorns, M. S. (2005) Ionization of zwitterionic amine substrates bound to monomeric sarcosine oxidase. *Biochemistry 44*, 16866–16874.
38. Chothia, C. (1976) The nature of the accessible and buried surfaces in proteins. *J. Mol. Biol. 105*, 1–14.
39. Basran, J., Bhanji, N., Basran, A., Nietlispach, D., Mistry, S., Meskys, R., and Scrutton, N. S. (2002) Mechanistic aspects of the covalent flavoprotein dimethylglycine oxidase of *Arthrobacter globiformis* studied by stopped-flow spectrophotometry. *Biochemistry 41*, 4733–4743.
40. Heuts, D. P. H. M., van Hellemond, E. W., Janssen, D. B., and Fraaije, M. W. (2007) Discovery, characterization, and kinetic analysis of an alditol oxidase from *Streptomyces coelicolor*. *J. Biol. Chem. 282*, 20283–20291.
41. Kow, R. L., Whicher, J. R., McDonald, C. A., Palfey, B. A., and Fagan, R. L. (2009) Disruption of the proton relay network in the class 2 dihydroorotate dehydrogenase from *Escherichia coli*. *Biochemistry 48*, 9801–9809.